Si vacancies in the 10-Å phase

M.D. WELCH,[1,2,]* A.R. PAWLEY,[3] S.E. ASHBROOK,[2] H.E. MASON,[4] AND B.L. PHILLIPS[4]

[1]Department of Mineralogy, The Natural History Museum, London SW7 5BD, U.K.
[2]Department of Earth Sciences, Cambridge University, Cambridge CB2 3EQ, U.K.
[3]School of Earth, Atmospheric and Environmental Sciences, The University of Manchester, Manchester M13 9PL, U.K.
[4]Department of Geosciences, SUNY Stony Brook, Stony Brook, New York 11794-2100, U.S.A.

ABSTRACT

^{29}Si MAS NMR spectroscopy on samples of 10-Å phase synthesized from oxides (6.0 GPa/600 °C/400 h) and from partial transformation of talc (6.5 GPa/650 °C/12.5 h) reveals that this phase contains Q^2-type Si sites in a ratio Q^3:Q^2 of 5.33:1. It is proposed that the Q^2 arise from adjacent vacancies in the tetrahedral sheets for which charge balance is most likely achieved by hydroxylation via a hydrogarnet-like substitution involving the formation of Q^2 silanol groups. Variable-contact-time ^{29}Si {^{1}H} CP/MAS NMR spectra of the talc/10-Å phase product support the assignment of Q^2 Si to the proposed $SiO_3(OH)$ groups. Electron microprobe analysis, including oxygen, gives the following empirical formula normalized to three Mg apfu and inferring a hydrogarnet component Si → 4H associated with Si vacancies: $Mg_3Si_{3.83(8)}O_{9.32}(OH)_{2.68} \cdot 1.1(4)H_2O$. The observed Mg:Si indicates a significant Si deficiency relative to talc. Comparison of the ^{29}Si MAS NMR and microprobe data indicates that Si vacancies likely occur as single isolated entities, rather than as pairs or clusters, and that between 1 in 18 and 1 in 23 Si sites is vacant. The results suggest new and intriguing possibilities for the incorporation of excess H into the 10-Å phase and, potentially, other phyllosilicates under upper-mantle conditions.

Keywords: 10-Å phase, Si vacancies, ^{29}Si NMR spectroscopy, silanol

INTRODUCTION

The 10-Å phase, nominally $Mg_3Si_4O_{10}(OH)_2 \cdot xH_2O$, is a synthetic dense hydrous magnesium silicate that has been proposed as a storage site for H_2O in subducting slabs (Thompson 1992), where it would form from talc at 4–5 GPa and remain stable to at least 7 GPa (Pawley and Wood 1995). Chinnery et al. (1999) observed by synchrotron powder X-ray diffraction the in situ transformation of talc to 10-Å phase in 20 min at 6 GPa/500 °C. Although numerous studies of the 10-Å phase have been made since its discovery forty years ago by Sclar et al. (1965), its structure (no H atom coordinates reported) was first determined recently by Comodi et al. (2005). The only published chemical analyses are given by Pawley et al. (1995) for a sample synthesized from talc + H_2O at 6.8 GPa, 650 °C, 44 h for which (Mg + Fe):Si = 3.02:3.99. Widely varying interlayer H_2O contents $^2/_3 < xH_2O < 2$ pfu have been reported. The X-ray structure reported by Comodi et al. (2005) has $x = 1$.

Spectroscopic studies of the 10-Å phase have led to some conflicting peak assignments and interpretations of OH environments (Bauer and Sclar, 1981; Fumagalli et al. 2001; Parry et al. in review), particularly distinguishing OH stretching modes of H_2O and structural OH. There is also considerable uncertainty about the range and nature of hydrogen-bonded interactions in the 10-Å phase, which bear upon the interpretation of vibrational spectra. The variable results of these studies may reflect a range of compositions and/or structural states for the 10-Å phase produced from different starting materials, *P-T* conditions and run durations. Here, we present new compositional and spectroscopic data that indicate the presence of Si vacancies in the tetrahedral sheet of the 10-Å phase and suggest new possibilities for compositional variation.

EXPERIMENTAL METHODS

Direct synthesis of deuterated 10-Å phase

Our original purpose in synthesizing deuterated 10-Å phase was to carry out a neutron powder diffraction study (Pawley et al., 2004). Deuterated 10-Å phase was synthesized from a 3:4 mixture of synthetic deuterated brucite, $Mg(OD)_2$, and SiO_2 glass. The starting mixture (0.120 g) was sealed in a Pt capsule with 9 wt% excess D_2O. The additional D_2O was added to ensure water-saturation for a possible deuterated 10-Å phase composition of $Mg_3Si_4O_{10}(OD)_2 \cdot 2D_2O$. Brucite was used in the starting material to eliminate the need to load a large volume of D_2O. A neutron-diffraction study of the bulk $Mg(OD)_2$ brucite sample synthesized at 0.1 GPa/500 °C (70 h) from which our starting material was taken determined a D content of 88 at%. The successful synthesis experiment (see below) was performed at 6.5 GPa/600 °C and lasted 400 h. The weight loss on puncturing the capsule after the experiment was ~2%.

Four syntheses were performed in a Walker-type multi-anvil apparatus at the University of Manchester under similar conditions. Owing to possible thermal gradients along the capsule length, each synthesis product was divided into three pieces corresponding to the top, middle, and bottom thirds, and then examined by powder X-ray diffraction for purity. Only the top and middle of the third synthesis (run DTAP3) gave XRD-pure 10-Å phase. This sub-sample amounted to 0.09 g. Most crystals from this sample (Fig. 1 inset) have subhedral hexagonal shapes and are thin (<15 μm), but some reach diameters of up to 0.25 mm, characteristically forming flat, highly reflective plates.

Powder X-ray diffraction data for the refinement of unit-cell parameters (Fig. 1) were collected for the entire 0.09 g sample (Enraf-Nonius position-sensitive detector, Cu$K\alpha_1$, 45 kV/40 mA). All peaks correspond to 10-Å phase and were indexed ab initio using the Crysfire2002 program suite (Shirley 2002) for a monoclinic 1M structure (Comodi et al. 2005). Refinement of 30 peak positions in the range of

* E-mail: mdw@nhm.ac.uk

6–80° 2θ gave a = 5.3297(9) Å, b = 9.205(3) Å, c = 10.202(3) Å, β = 100.08(2)°, V = 492.8(2) Å^3. Cell parameters were also obtained for three single crystals of 10-Å phase from DTAP3 (CAD4 and Xcalibur diffractometers, Mo$K\alpha$, 45 kV/40 mA): a = 5.3052(8)/5.306(1)/5.3057(9) Å, b = 9.187(1)/9.193(3)/9.178(2) Å, c = 10.172(2)/10.192(4)/10.166 Å, β = 100.03(2)/100.05(4)/99.96(3)°, V = 488.2(1)/489.5(3)/487.6(2) Å^3. The d_{001} values for these three crystals are 10.017, 10.036, and 10.013 Å, respectively. Thus, different crystals have similar cell parameters and confirm that sample DTAP3 is homogeneous and demonstrably a 10-Å phase. A structure solution and refinement of the crystal shown in Figure 1 (lower inset photo) was made for which full experimental details and results will be reported in a separate paper. Our sample and that of Comodi et al. (2005) have essentially the same X-ray characteristics and structure.

Synthesis of deuterated 10-Å phase by transformation of talc

A second sample of 10-Å phase (HM-338) was produced from partially transformed talc + D$_2$O at 6.5 GPa, 650 °C (12.5 h). The talc (26.3 mg) and D$_2$O (8 μL) were loaded into a silver capsule and sealed by a press-fit cap. Pressure was applied by a 1000 ton Kennedy-Walker type uniaxial split-cylinder multi-anvil press (USCA-1000) at SUNY Stony Brook. Partial decompression during the run from 6.5 to 5.1 GPa resulted in a mixture of talc and 10-Å phase. The powder X-ray diffraction pattern of HM-338 is shown in Figure 1, from which it is evident that the 10-Å phase produced is well crystallized (sharp basal reflections) and compares closely with the pattern of DTAP3.
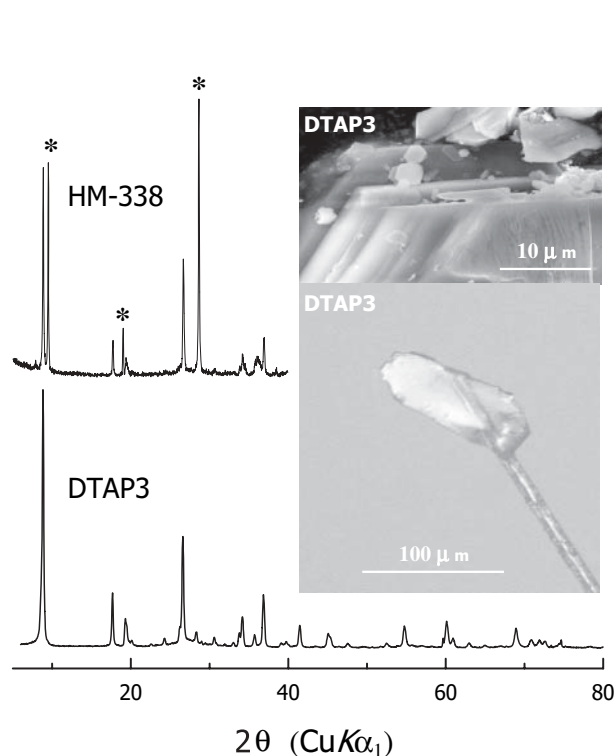
Electron microprobe analysis of DTAP3 crystals

Electron microprobe analysis (EMPA) of 10-Å phase single crystals from sample DTAP3 was performed using a Cameca SX100 EMP operated at 10 kV and 40 nA in wavelength-dispersive mode (WDS) with a 7 μm beam. Pure, low-Fe natural talc was used as a suitable standard for comparison. Element standards used for talc and 10-Å phase were synthetic end-member forsterite (O$K\alpha$), periclase (Mg$K\alpha$), wollastonite (Si$K\alpha$), and natural St John's Rocks olivine (Fe$K\alpha$). The two larger crystals of 10-Å-phase from sample DTAP3 for which unit-cell data were obtained were mounted on a glass slide with their (001) faces parallel to the slide surface and carbon-coated.

^{29}Si NMR spectroscopy

NMR experiments were performed in two different laboratories. ^{29}Si MAS NMR spectroscopy on DTAP3 was performed at Cambridge University (Earth Sciences) using a 400 MHz (9.4 T) Chemagnetics Infinity spectrometer operating at 79.5 MHz. The powdered sample was packed inside a 4 mm rotor and spun at 7 kHz. A radio-frequency field strength, ω$_1$/2π, of 90 kHz and a conventional single-pulse experiment were used. Recycle intervals were optimized as far as possible to ensure the relative intensities of peaks within the same spectrum were consistent. A total of 668 acquisitions with a 120 s recycle interval were
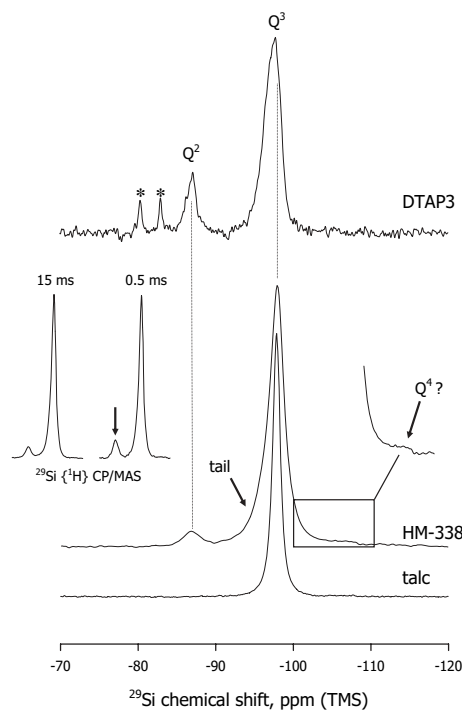

FIGURE 1. Powder X-ray diffraction patterns (Cu$K\alpha_1$ radiation) of the DTAP3 sample and the HM-338 talc/10-Å mixture, with diagnostic talc peaks shown by asterisks. For DTAP3, only peaks from the 10-Å phase are present, whereas HM-338 is clearly a mixture of talc and the 10-Å phase. Photos: representative images of 10-Å phase crystals from sample DTAP3. The upper image is a SEM micrograph and shows numerous euhedral tiny crystallites. The lower image is a photomicrograph of a crystal mounted on a thin X-ray transparent carbon fiber.

FIGURE 2. Top: ^{29}Si MAS NMR spectrum of sample DTAP3: the two weak peaks indicated by asterisks are due to a minor clinoenstatite impurity. Bottom: ^{29}Si {^{1}H} CP/MAS NMR spectrum of the talc starting material used in the synthesis of HM-338. Middle: ^{29}Si MAS NMR spectrum of a partially transformed mixture of talc and the 10-Å phase. Insets: CP/MAS spectra of HM-338 collected using contact times of 0.5 and 15 ms. Preferential enhancement of the Q^2 peak at the shorter contact time is evident (arrowed). An enlarged inset of the –100 to –110 ppm part of the HM-338 spectrum relating to a possible Q^4 peak is shown with the vertical scale doubled to make the feature clearer.

collected. A pulse flip angle of $\pi/4$ was used. Computer-simulated fits were obtained using the DMFIT program (Massiot et al. 2002). ^{29}Si NMR spectra of sample HM-338 were obtained at SUNY Stony Brook with a 400 MHz (9.4 T) Varian Inova spectrometer operating at 79.4 MHz for ^{29}Si and 399.76 MHz for ^{1}H and using a Varian/Chemagnetics T3 probe assembly configured for 3.2 mm (o.d.) rotors. Single-pulse experiments used 5 μs pulses ($\pi/2 = 6$ μs) and a 150 s recycle delay at a spinning rate of 12 kHz. The ^{29}Si{^{1}H} CP/MAS spectra were collected at a spinning rate of 5 kHz using a linear $\nu_{1,H}$ ramp of ±5 kHz about $\nu_{1,H} = 42$ kHz. In this paper we follow the conventional NMR notation for Si peaks: Q^n corresponds to a tetrahedral Si with n tetrahedrally coordinated next-nearest neighbors. As all n are Si in the 10-Å phase, we do not need to qualify Q^n further [e.g., Q^n(0Al), Q^n(1Al), etc]. All chemical shifts reported are referenced to tetramethylsilane (TMS).

RESULTS AND DISCUSSION

Electron microprobe analysis of DTAP3: Mg, Si, O

The average composition (wt%) of 10 analyses of the talc standard sample is Mg 18.50(2), Fe 0.38(7), Si 29.2(1), O 47.6(4). The corresponding average Mg:Si normalized to O = 12 apfu (atoms per formula unit) is 3.07(4):4.03(4), being essentially that of the ideal end-member composition. The oxygen contents normalized to Mg = 3 and Si = 4 apfu are 11.74(16) and 11.47(6) apfu, respectively, corresponding to small oxygen deficits of 2% and 4%. The talc data serve as a good index of the experimental uncertainties on Mg, Si, and O analysis obtained by electron microprobe in this study. The average Si and O contents of 10-Å phase (DTAP3) obtained from 31 analyses of the two crystals and normalized to Mg = 3 apfu are Si = 3.83(8) apfu and O = 13.13(36) apfu. The errors (2σ) on these values include an error propagated from that of the average Mg value. The Mg/Si of 0.784(16) compared with 0.761(9) determined for talc demonstrates that the 10-Å phase is Si-deficient compared with talc. The significance of these results is discussed below in the light of our NMR study. The oxygen content of the 10-Å phase determined by EMPA indicates that the interlayer molecular H_2O content x is $0.7 < x < 1.5$ pfu. This range would seem to rule out the value of $x = 2$ proposed in some studies (Yamamoto and Akimoto 1977; Pawley and Wood 1995). The average value is close to $x = 1$ pfu and corresponds to that determined from X-ray site-scattering by Comodi et al. (2005). Thus, there is independent agreement on the interlayer H_2O content being consistent with 1 H_2O pfu.

^{29}Si NMR spectra

The ^{29}Si MAS NMR spectrum of DTAP3 (Fig. 2) has peaks at –97.6, –87.1, –83.1, and –80.4 ppm with best-fit intensity ratios of 80:15:2.5:2.5. The chemical shifts indicate that the –97.6 ppm peak is related to Q^3 and the other peaks are Q^2. The Q^3 peak at –97.6 ppm is close to that of talc, –98.1 ppm (Lippmaa et al. 1980), and its FWHM of 3 ppm is typical of many phyllosilicates (e.g., Barron and Frost 1985; Kinsey et al. 1985). The two weak Q^2 peaks of equal intensity at –83.1 and –80.4 ppm are related to a minor low-clinoenstatite (Janes and Oldfield 1985) impurity that is not registered by powder X-ray diffraction. Recycle delays of between 1 s and 3 min were used to check for differential relaxation of Q^2 and Q^3 peaks, and none was observed. The spectrum

of DTAP3 is almost identical, except for the clinoenstatite peaks, to that reported by Kohn and Fumagalli (2002) for the same bulk 10-Å phase sample synthesized at 6.7 GPa/650 °C/360 h from which the crystal described by Comodi et al. (2005) was taken (S.C. Kohn, personal communication). In that spectrum the Q^3 and Q^2 peaks occur in almost the same ratio (5.67:1) as they do in DTAP3 (5.33:1). The absence of differential relaxation we observe for these two peaks also supports their assignment to the same phase.

The ^{29}Si MAS NMR spectrum of HM-338 (Fig. 2) contains two distinct peaks with chemical shifts of –98.0 and –86.9 ppm and intensity ratio 24:1. The –98 ppm peak, assigned to Q^3, is clearly asymmetric with a tail towards less negative chemical shifts. The –86.9 ppm peak has almost the same chemical shift as the Q^2 peak of the DTAP3 spectrum (–87.1 ppm) and is assigned to the 10-Å phase. Fitting of the spectrum indicates that the asymmetric Q^3 peak has two components at –98.0 (talc) and –97.6 ppm, the latter being close to the Q^3 peak in the DTAP3 spectrum and so is also assigned to the 10-Å phase. The intensity ratio of the three peaks Q^3 (talc): Q^3 (10-Å): Q^2 (10-Å) is 75:21:4. Comparison of the spectrum of HM-338 with the ^{29}Si {^{1}H} CP/MAS spectrum of the talc starting material (Fig. 2) shows that Q^2 sites are produced in the formation of the 10-Å phase. A fourth very minor feature at around –106 ppm in the ^{29}Si MAS NMR spectrum of HM-338 (Fig. 2 enlarged inset) is likely Q^4, but cannot be assigned to any known crystalline phase in the MSH system, and so may be amorphous silica. It is possible, if not likely, that the occurrence of this minor silica-rich phase arises from the reduced Si content of the 10-Å phase relative to talc. The Q^3:Q^2 ratio of the two peaks assigned to the 10-Å phase is 5.25:1 and agrees well with that determined for the DTAP3 sample (5.33:1). Variable-contact-time ^{29}Si {^{1}H} CP/MAS NMR spectra of HM-338 (Fig. 2) show an enhancement of the Q^2 peak relative to the combined Q^3 peak at short contact time. This observation indicates stronger Si-H dipolar coupling for Q^2, consistent with protonation of the broken Si-O-Si linkage upon vacancy formation, resulting in silanol groups.

The occurrence of Q^2 Si as silanol groups at the edges of crystals of extremely thin fibrous crystallites of sepiolite and palygorskite has been observed by ^{29}Si MAS NMR (Barron and Frost 1985). However, even for these fibers (diameters of <10 nm), NMR indicates Q^3:Q^2 intensity ratios of more than 20:1. Thus, Q^2 groups at crystal edges have a small, albeit potentially detectable, ^{29}Si -NMR signature. As stated above, most of the crystals of the 10-Å phase in sample DTAP3 are euhedral or subhedral for a wide range of sizes. A simple geometrical calculation for such crystals shows that the observed Q^3:Q^2 ratio of 5.33 implies an *average maximum* crystallite diameter of only 4 nm, which is far smaller than the *minimum* crystal size observed by scanning-electron microscopy (~200 nm for DTAP3 and ~100 μm for HM-338). We conclude that the –87.1 ppm peak is not related to Q^2 at crystal edges, nor to any impurity phase—it is from the 10-Å phase.

The agreement between the ^{29}Si NMR spectra presented here and those of Kohn and Fumagalli (2002), and with samples prepared from oxides or talc starting materials with run durations ranging from 12.5–400 h, shows that the 10-Å phase has a reproducible structure characterized by the presence of Q^2 Si

sites. Considering these various observations, we infer that the 10-Å phase has Si vacancies within its tetrahedral sheets. If the Si vacancies were to occur as single isolated entities, each surrounded by three Q^2, then the Q^3:Q^2 ratio of 5.33:1 determined for our sample corresponds to 1 in 20 Si sites being vacant (16 Q^3 + 3 Q^2 + 1 vacancy) and an implied Si content of 3.80 apfu. This value is close to 3.83(8) Si pfu determined by EMPA for DTAP3. If the vacancies were to be paired (two Q^2 per vacancy), then a value of 3.70 Si apfu is implied, somewhat below that measured. Higher degrees of vacancy clustering imply lower Si contents. The estimated uncertainty on the simulation of the Q^3 and Q^2 peaks is ±2% absolute for DTAP3 (Fig. 2). Hence, the ^{29}Si MAS NMR spectrum constrains the proportion of vacant tetrahedral sites in DTAP3 quite tightly to be between 1 in 18 and 1 in 23 tetrahedra. We conclude that the 10-Å phase is significantly Si-deficient relative to talc, and that the observed Si content is consistent with the occurrence of isolated tetrahedral vacancies: the NMR data indicate that around one in twenty Si sites in the 10-Å phase is vacant.

How is the Si deficiency we observe for the 10-Å phase charge-balanced? The simple "MSH" composition does not leave many options for charge-balancing. No evidence has so far been found for hydronium H_3O^+ in the 10-Å phase (Fumagalli et al. 2001). Infrared and Raman spectroscopy on DTAP3 (Pawley et al. in preparation) also exclude the presence of hydronium. The only remaining option would seem to be to protonate the "dangling" Si-O bond of each of the three Q^2 Si, forming a $SiO_3(OH)$ group. Locally, charge-balance would also require protonation of the $^{[6]}$Mg-O oxygen that is normally bonded to Si, producing a $[MgOH\cdot3SiO_3(OH)]$ moiety. Silanol groups in minerals are not common, but the occurrence of $SiO_3(OH)$ groups is well established (Nyfeler and Armbruster 1998) and the energetics and crystal-chemical basis for stabilizing silanol groups as essential structural components, rather than just as features of crystal edges and surfaces, has been explored computationally (Gibbs 1982; Mortier et al. 1984).

In the hydrated 2:1 phyllosilicate shafranovskite (Krivovichev et al. 2004) more than half the Si of the tetrahedral sheets are $SiO_3(OH)$ Q^2 groups which occur in clusters. However, in shafranovskite the $SiO_3(OH)$ triplet of Si3 atoms is not associated with a vacant tetrahedral site and so is not directly analogous to a hydrogarnet-type group such as the $[MgOH\cdot3SiO_3(OH)]$ moiety proposed here for the 10-Å phase. The distinctive feature of the Q^2 groups in the 10-Å phase is, we propose, their likely occurrence as $SiO_3(OH)$ triplets around isolated tetrahedral vacancies. A further point relating to H_2O incorporation is that normally the talc interlayer is hydrophobic (Wang et al. 2005), but the presence of silanols in the 10-Å phase provides a mechanism for bonding interlayer water to the tetrahedral sheet.

The data reported in this paper reveal a significant, previously unrecognized, feature of the 10-Å phase: the presence of vacancies in the tetrahedral sheet and their likely association with silanols. The proportion of vacancies inferred from the NMR data is around 5 % and so is likely to have a weak expression in X-ray diffraction and, we suggest, has passed undetected. Our results indicate new and intriguing possibilities for the incorporation of excess H into the 10-Å phase and, perhaps, into other phyllosilicates at P-T conditions of the upper mantle.

REFERENCES CITED

Barron, P.F. and Frost, R.L. (1985) Solid-state ^{29}Si NMR examination of the 2:1 ribbon magnesium silicates, sepiolite, and palygorskite. American Mineralogist, 70, 758–766.

Bauer, J.F. and Sclar, C.B. (1981) The "10Å phase" in the system MgO-SiO$_2$-H$_2$O. American Mineralogist, 66, 576–585.

Chinnery, N.J., Pawley, A.R., and Clark, S.M. (1999) In situ observation of the formation of 10 Å phase from talc + H$_2$O at mantle pressures and temperatures. Science, 286, 940–942.

Comodi, P., Fumagalli, P., Nazzareni, S., and Zanazzi,, P.F. (2005) The 10 Å phase: Crystal structure from single-crystal X-ray data. American Mineralogist, 90, 1012–1016.

Fumagalli, P., Stixrude, L., Poli, S., and Snyder, D. (2001) The 10 Å phase: a high-temperature expandable phyllosilicate stable during subduction of hydrated lithosphere. Earth and Planetary Science Letters, 186, 125–141.

Gibbs, G.V. (1982) Molecules as models for bonding in silicates. American Mineralogist, 67, 421–450.

Janes, N. and Oldfield, E. (1985) Prediction of silicon-29 NMR chemical shifts using a group-electronegativity approach: applications to silicate and aluminosilicate structures. Journal of the American Chemical Society, 107, 6769–6775.

Kinsey, R.A., Kirkpatrick, R.J., Hower, J., Smith, K.A., and Oldfield, E. (1985) High-resolution aluminium-27 and silicon-29 nuclear magnetic resonance spectroscopic study of layer silicates, including clay minerals. American Mineralogist, 70, 537–548.

Kohn, S.C. and Fumagalli, P. (2002) New constraints on the structure of 10 Å phase from ^{1}H and ^{29}Si MAS NMR data. Abstract WP16, 18th EMPG meeting, Edinburgh, U.K.

Krivovichev, S.V., Yakovenchuk, V.N., Armbruster, T., Pakhomovsky, Y.A., Weber, H.-D., and Depmeier, W. (2004) Synchrotron X-ray diffraction study of the structure of shafranovskite, K$_2$Na$_3$(Mn,Fe,Na)$_4$[Si$_9$(O,OH)$_{27}$](OH)$_2$·nH$_2$O, a rare manganese phyllosilicate from the Kola peninsula, Russia. American Mineralogist, 89, 1816–1821.

Lippmaa, E., Mägi, M., Samoson, A., Engelhardt, G., and Grimmer, A-R. (1980) Structural studies of silicates by solid-state high-resolution ^{29}Si NMR. Journal of the American Chemical Society, 102, 4889–4893.

Massiot, D., Fayon, F., Capron, M., King, I., Le Calvé, S., Alonso, B., Durand, J-O., Bujoli, B., Gan, Z., and Hoatson, G. (2002) Modelling one- and two-dimensional solid-state NMR spectra. Magnetic Resonance in Chemistry, 40, 70–76.

Mortier, W.J., Sauer, J., Lercher, J.A., and Noller, H. (1984) Bridging and terminal hydroxyls. A structural chemical and quantum chemical discussion. Journal of Physical Chemistry, 88, 905–912.

Nyfeler, D. and Armbruster, T. (1998) Silanol groups in minerals and inorganic compounds. American Mineralogist, 83, 119–125.

Pawley, A.R. and Wood, B.J. (1995) The high-pressure stability of talc and 10-Å phase: storage sites for H$_2$O in subduction zones. American Mineralogist, 89, 998–1003.

Pawley, A.R., Redfern, S.A.T., and Wood, B.J. (1995) Thermal expansivities and compressibilities of hydrous phases in the system MgO-SiO$_2$-H$_2$O; talc, phase A and the 10-Å phase. Contributions to Mineralogy and Petrology, 122, 301–307.

Pawley, A.R., Welch, M.D., and Smith, R.I. (2004) The 10-Å phase: structural constraints from neutron powder diffraction. Lithos, 73, 1–2 (S86).

Sclar, C.B., Carrison, L.C., and Schwartz, C.M. (1965) High-pressure synthesis and stability of a new hydronium-bearing layer silicate in the system MgO-SiO$_2$-H$_2$O. Transactions of the American Geophysical Union, 46, 184.

Shirley, R. (2002) The Crysfire 2002 system for automatic powder indexing. User Manual. http://www.ccp14.ac.uk/tutorial/crys/program/crysfire.htm

Thompson, A.B. (1992) Water in the Earth's upper mantle. Nature, 385, 288–312.

Wang, J.W., Kalinichev, A.G., and Kirkpatrick, R.J. (2005) Structure and decompression melting of a novel, high-pressure nanoconfined 2-D ice. Journal of Physical Chemistry B, 109, 14308–14313.

Yamamoto, K. and Akimoto, S. (1977) The system MgO-SiO$_2$-H$_2$O at high pressures and temperatures—the stability field for hydroxyl chondrodite, hydroxyl clinohumite, and 10Å phase. American Journal of Science, 277, 288–312.